JOURNAL OF VIROLOGY, Jan. 2010, p. 153–162 Vol. 84, No. 1
0022-538X/10/$12.00 doi:10.1128/JVI.01447-09

Effects of Phosphorylation of Herpes Simplex Virus 1 Envelope Glycoprotein B by Us3 Kinase In Vivo and In Vitro▽

Takahiko Imai,[1] Ken Sagou,[1,2] Jun Arii,[1] and Yasushi Kawaguchi[1]*

Division of Viral Infection, Department of Infectious Disease Control, International Research Center for Infectious Diseases, The Institute of Medical Science, The University of Tokyo, Minato-ku, Tokyo 108-8639,[1] and Nippon Institute for Biological Science, Ome, Tokyo 198-0024,[2] Japan

Received 14 July 2009/Accepted 12 October 2009

We recently reported that the herpes simplex virus 1 (HSV-1) Us3 protein kinase phosphorylates threonine at position 887 (Thr-887) in the cytoplasmic tail of envelope glycoprotein B (gB) (A. Kato, J. Arii, I. Shiratori, H. Akashi, H. Arase, and Y. Kawaguchi, J. Virol. 83:250–261, 2009; T. Wisner, C. C. Wright, A. Kato, Y. Kawaguchi, F. Mou, J. D. Baines, R. J. Roller and D. C. Johnson, J. Virol. 83:3115–3126, 2009). In the studies reported here, we examined the effect(s) of this phosphorylation on viral replication and pathogenesis in vivo and present data showing that replacement of gB Thr-887 by alanine significantly reduced viral replication in the mouse cornea and development of herpes stroma keratitis and periocular skin disease in mice. The same effects have been reported for mice infected with a recombinant HSV-1 carrying a kinase-inactive mutant of Us3. These observations suggested that Us3 phosphorylation of gB Thr-887 played a critical role in viral replication in vivo and in HSV-1 pathogenesis. In addition, we generated a monoclonal antibody that specifically reacted with phosphorylated gB Thr-887 and used this antibody to show that Us3 phosphorylation of gB Thr-887 regulated subcellular localization of gB, particularly on the cell surface of infected cells.

The herpes simplex virus 1 (HSV-1) Us3 gene encodes a serine/threonine protein kinase with an amino acid sequence that is conserved in the subfamily *Alphaherpesvirina*e (9, 20, 29). The Us3 kinase phosphorylation target site has been reported to be similar to that of protein kinase A (PKA), a cellular cyclic AMP-dependent protein kinase (3, 12). Us3 catalytic activity plays important roles in viral replication and pathogenesis in vivo, based on studies showing that recombinant Us3 null mutant viruses and recombinant viruses encoding catalytically inactive Us3 have significantly reduced virulence, pathogenicity, and replication in mouse models (21, 34). In contrast, Us3 is not essential for growth in tissue culture cells (29). Thus, recombinant Us3 mutants grow as well as wild-type virus in Vero cells and have modestly impaired growth in a specific cell line such as HEp-2 cells (32, 33). The catalytic activity of Us3 is, in part, regulated by autophosphorylation of its serine at position 147 (Ser-147), and regulation of Us3 activity by autophosphorylation of Ser-147 appears to play a critical role in HSV-1 replication in vivo and in HSV-1 pathogenesis (34). Numerous studies have elucidated the potential downstream effects of Us3, including blocking apoptosis (18, 26–28), promoting nuclear egress of progeny nucleocapsids through the nuclear membrane (24, 32, 33), redistributing and phosphorylating nuclear membrane-associated viral nuclear egress factors UL31 and UL34 (13, 24, 30, 31) and cellular proteins including lamin A/C and emerin (16, 22, 23), controlling infected cell morphology (12, 27), and downregulating cell surface expression of viral envelope glycoprotein B (gB) (11).

Two substrates that mediate some of the Us3 functions described above have been identified. First, it has been shown that Us3 phosphorylates Thr-887 in the cytoplasmic tail of gB, which appears to downregulate cell surface expression of gB (11). This conclusion is based on the observation that a T887A mutation in gB (gB-T887A) markedly upregulated cell surface expression of gB in infected cells: this upregulation was also observed with a recombinant virus encoding a Us3 kinase-inactive mutant, whereas a phosphomimetic substitution for gB Thr-887 restored wild-type cell surface expression of gB (11). Us3 phosphorylation of gB Thr-887 has also been proposed to be involved in regulation of fusion of the nascent progeny virion envelope with the cell's outer nuclear membrane, based on the observation that virions accumulated aberrantly in the perinuclear space in cells infected with a mutant virus carrying the gB-T887A substitution mutation and lacking the capacity to produce gH (42). Second, it has been shown that Us3 may phosphorylate some or all of the six serines in the UL31 N-terminal region (24). Such phosphorylation might regulate proper localization of UL31 and UL34 at the nuclear membrane, nuclear egress of nucleocapsids, and viral growth in cell cultures since the Us3 kinase-inactive mutant phenotype for nuclear egress (i.e., mislocalization of UL31 and UL34 at the nuclear membrane, aberrant accumulation of virions within herniations of the nuclear membrane, and decreased viral growth in cell cultures) is also produced by replacement of the six serines in the UL31 N-terminal region with alanines while phosphomimetic substitutions of the six serines restored the wild-type phenotype (24).

Thus, the molecular mechanisms for some of the downstream effects of Us3 phosphorylation have been gradually elucidated. However, it remains to be shown whether the Us3

* Corresponding author. Mailing address: Division of Viral Infection, Department of Infectious Disease Control, International Research Center for Infectious Diseases, The Institute of Medical Science, The University of Tokyo, 4-6-1 Shirokanedai, Minato-ku, Tokyo 108-8639, Japan. Phone: 81 3 6409 2070. Fax: 81 3 6409 2072. E-mail: ykawagu@ims.u-tokyo.ac.jp.

▽ Published ahead of print on 21 October 2009.

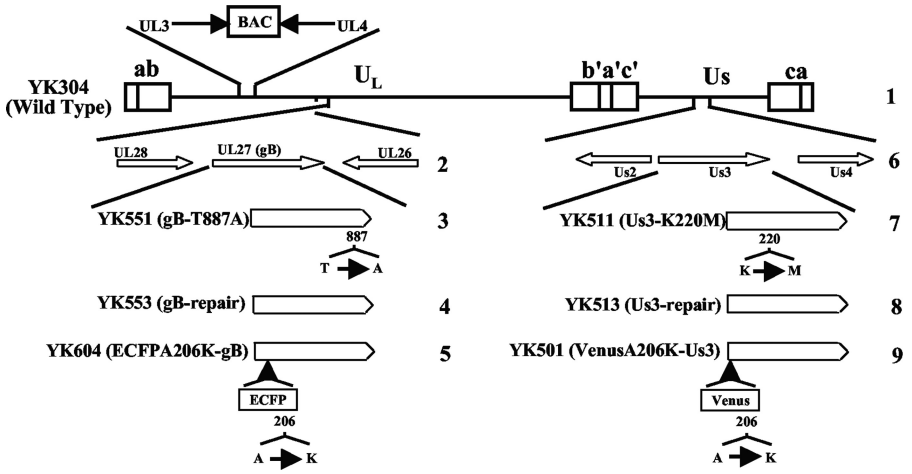

FIG. 1. Schematic diagram of the genome structure of wild-type virus YK304 and the relevant domains of the recombinant viruses in this study. Line 1, linear representation of the YK304 genome. Unique sequences are represented as unique long (U_L) and short (U_S) domains, and the terminal repeats flanking them are shown as open rectangles with the designation above each repeat. The YK304 genome has a bacmid (BAC) in the intergenic region between UL3 and UL4. Line 2, domains encoding the UL26, UL27 (gB), and UL28 open reading frames. Line 6, domains encoding the Us2, Us3, and Us4 open reading frames. Lines 3, 4, 5, 7, 8, and 9, schematic diagrams of recombinant viruses YK551, YK553, YK604, YK511, YK513, and YK501, respectively.

functions reported to date are in fact involved in viral replication and pathogenicity in vivo. In the present study, we focused on Us3 phosphorylation of gB Thr-887 and examined the effect(s) of this phosphorylation on viral replication and pathogenesis in vivo. These studies have shown that replacement of gB Thr-887 by alanine significantly reduced viral replication in the mouse cornea and development of herpes stroma keratitis (HSK) and periocular skin disease in mice, as reported for infection of mice with a recombinant virus carrying a Us3 kinase-inactive mutant (34). These observations suggested that Us3 phosphorylation of gB Thr-887 played a critical role in viral replication in vivo and in HSV-1 pathogenesis. In addition, we generated a monoclonal antibody that specifically recognized phosphorylated gB Thr-887 and used this antibody to directly study the functional consequences of Us3 phosphorylation of gB Thr-887 in infected cells. We also present data showing that Us3 phosphorylation of gB Thr-887 regulated subcellular localization of gB, particularly gB localization on the cell surface of infected cells.

MATERIALS AND METHODS

Cells and viruses. Vero and rabbit skin cells were described previously (39). HSV-1 wild-type strain HSV-1(F) was described previously (39). Recombinant virus YK511, encoding an enzymatically inactive Us3 mutant in which lysine at Us3 position 220 was replaced with methionine (Us3-K220M); recombinant virus YK513, in which the Us3 K220M mutation in YK511 was repaired (Us3-KM-repair); recombinant virus YK551 with the gB-T887A mutation; and recombinant virus YK553, in which the gB-T887A mutation in YK551 was repaired (gB-repair), were described previously (Fig. 1) (11, 12). The maintenance of OriL in YK551 and YK553 was confirmed by a method described previously (39) (data not shown). Recombinant virus YK604 (ECFPA206K-gB) encoding gB fused to enhanced cyan fluorescent protein carrying the mutation A206K (ECFPA206K) was described previously (Fig. 1) (38). Recombinant virus YK304, the parent virus of the recombinant viruses described above, was reconstituted from pYEbac102 containing a complete HSV-1(F) sequence with the bacterial artificial chromosome sequence inserted into the HSV intergenic region between UL3 and UL4 (39) (Fig. 1). YK304 has been shown to have the same phenotype in cell cultures and in mouse models (39). Recombinant virus YK501 (VenusA206K-Us3) encoding Us3 fused to the fluorescent protein Venus with the A206K mutation (VenusA206K) (Fig. 1) was generated by cotransfection of rabbit skin cells with transfer plasmid pBS-VenusA206K-Us3 (12) and intact YK304 viral DNA, purified on 5 to 20% potassium acetate gradients, and screened for fluorescent plaques as described previously (38).

Antibodies and chemicals. Mouse monoclonal antibodies to gB (1105) and ICP0 (1112) were purchased from the Goodwin Institute. Mouse monoclonal antibody to α-tubulin (DM1A) was purchased from Sigma-Aldrich. Rabbit polyclonal antibodies to lamin B1, pan-cadherin, and CD71 were purchased from Abcam. Rabbit polyclonal antibodies to protein disulfide isomerase (PDI), the α-subunit of eukaryotic initiation factor 2 (eIF-2α), and early endosome antigen 1 were purchased from StressGen, Santa Cruz Biotechnology, and Cell Signaling Technology, respectively. Anti-phospho-eIF-2α was purchased from StressGen. Mouse monoclonal antibodies that recognize gB with phosphorylated Thr-887 (gB-T887^P) were generated as described previously (34), except that peptides corresponding to gB residues 881 to 893 (MRKRRNTNYTQVP) with and without phosphorylated Thr-887 were used (purchased from GL Biochem). Thapsigargin was purchased from Sigma-Aldrich.

Immunoblotting, immunofluorescence, and immunoprecipitation. Immunoblotting was performed as described previously (14), except that Can Get Signal Immunoreaction Enhancer Solution (Toyobo) was used when membranes were probed with monoclonal antibody to gB-T887^P. The amount of protein in the bands was quantitated using the Dolphin Doc image capture system with Dolphin-1D software (Wealtec). Indirect immunofluorescence was performed as described previously (1) except that Can Get Signal Immunostain solution A (Toyobo) was used. Immunoprecipitation was performed as described previously (34).

Phosphatase treatment. Lysates of HSV-1(F)-infected Vero cells were treated with λ phosphatase as described previously (34).

Purification of virions. Virions were purified as described previously (40).

Animal studies. Female ICR mice were purchased from Charles River. For intracerebral infection, 3-week-old female mice were infected with 10-fold serial dilutions of each HSV-1 strain, as described previously (39). Mice were monitored daily, and mortality from 1 to 14 days postinfection was attributed to the inoculated viruses. The 50% lethal dose (LD_{50}) values were calculated by the Behrens-Karber method. For ocular infection, 5-week-old female mice were infected with each HSV-1 strain as described previously (34). The scoring scale for the severity of HSK and periocular skin disease was described previously (34), and scoring was done blind. Viral titers in tear films were determined as described previously (34). All animal studies were carried out with the approval of the Ethical Committee for Animal Experimentation at the University of Tokyo.

Endocytosis of gB assayed by biotinylation in infected cells. Endocytosis of gB in infected cells was assayed as described previously (19) with minor modifications. Briefly, Vero cells were infected with wild-type HSV-1(F) at a multiplicity of infection (MOI) of 1 for 18 h, and the cells were then biotinylated for 15 min

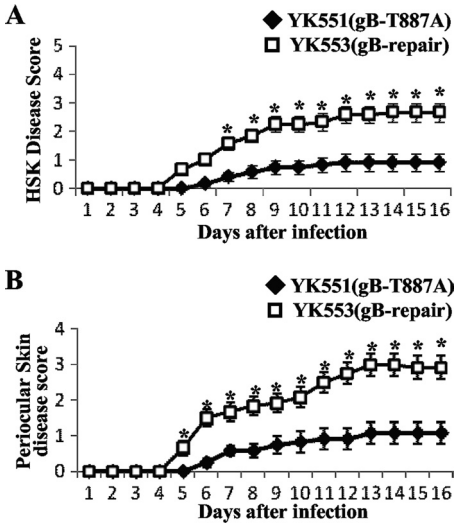

FIG. 2. Effect of the gB-T887A mutation on HSK and periocular skin disease in mice. Twelve 5-week-old female ICR mice were infected with 1×10^6 PFU of YK551 (gB-T887A) or YK553 (gB-repair) by corneal scarification and scored for HSK (A) and periocular skin disease (B) every other day for 16 days. The data shown are the averages and standard errors of the observations. A statistically significant difference between HSK and periocular skin disease scores in mice infected with YK551 (gB-T887A) and those infected with YK553 (gB-repair) was noted (*, $P < 0.01$).

at 4°C by using cleavable sulfo-NHS-SS-biotin [sulfosuccinimidyl 2-(biotinamido)-ethyl-1,3-dithiopropionate; Pierce]. After extensive washes, cells were incubated at 37°C for 0 or 4 h to allow endocytosis of the biotinylated cell surface proteins. The cells were then treated twice with freshly prepared reducing solution (15.5 mg of glutathione/ml, 75 mM NaCl, 0.3% NaOH, 10% calf serum) at 4°C to remove any remaining biotin label from proteins present at the cell surface. After extensive washes and quenching free sulfhydryl groups with 5 mg/ml of iodoacetamide in phosphate-buffered saline containing 1% bovine serum albumin, the cells were harvested, solubilized, and immunoprecipitated with anti-gB or anti-gB-T887^P antibody and analyzed by immunoblotting with streptavidin-horseradish peroxidase or anti-gB antibody.

RESULTS

Effect of the gB-T887A mutation on viral replication and pathogenesis in mice. To determine the effect of the gB-T887A mutation on viral replication and pathogenesis in vivo, we employed two murine models of HSV-1 infection. We recently reported that mice infected with YK511 (Us3-K220M) exhibited reduced severity of HSK and periocular skin disease compared to mice infected with YK513 (Us3-repair), and that YK511 (Us3-K220M) replicated significantly less efficiently than YK513 (Us3-repair) in the tear films of these infected mice (34). Therefore, in the first series of experiments, 5-week-old female ICR mice were inoculated ocularly with 1×10^6 PFU/eye of YK551 carrying gB-T887A or of YK553 in which the gB-T887A mutation in YK551 was repaired (gB-repair). The inoculated mice were observed daily for development of HSK and periocular skin disease for 16 days postinfection. In addition, to examine viral replication at the infection site, tear film samples were collected at 1 and 5 days postinfection, and viral titers were determined. In this study, mice infected with YK551 (gB-T887A) exhibited reduced severity of HSK and periocular skin disease compared to mice infected with YK553 (gB-repair) virus (Fig. 2). Similar results were obtained when mice were infected ocularly with 1×10^5 PFU of each of the viruses (data not shown). In addition, YK551 (gB-T887A) replicated significantly less efficiently than YK553 (gB-repair) in the tear films of these infected mice, with titers approximately seven- to eightfold lower than those of the repaired virus (Fig. 3). These results indicated that the Us3 phosphorylation site in gB (Thr-887) was required for efficient viral replication and for development of HSK and periocular skin disease in mice.

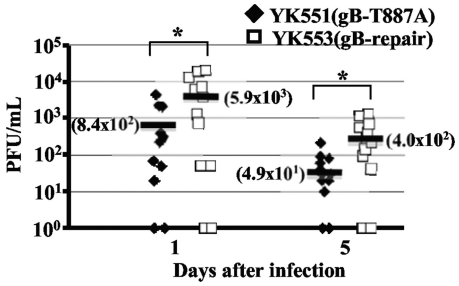

FIG. 3. Effect of the gB-T887A mutation on virus growth in the tear film of mice following corneal infection. In the experiment described in the legend of Fig. 2, viral titers in the tear films of infected mice at 1 and 5 days postinfection were determined by standard plaque assays. Each data point represents the titer in the tear film of one mouse. The horizontal bars and figures in the parentheses show the averages for each group. A statistically significant difference in viral titers between mice infected with YK551 (gB-T887A) and YK513 (gB-repair) was noted (*, $P < 0.05$).

In the second series of experiments, 3-week-old female ICR mice were infected intracerebrally with 10-fold-dilutions of YK511 (Us3-K220M), YK513 (Us3-repair), YK551 (gB-T887A), or YK553 (gB-repair), and mortality was monitored for 14 days postinfection. As shown in Table 1, the LD_{50} of YK511 (Us3-K220M) was 10^3-fold less than that of YK513 (Us3-KM-repair), indicating that HSV-1 Us3 kinase activity played a critical role in HSV-1 virulence in mice following intracerebral inoculation. These results are in agreement with an earlier report that an HSV-1 Us3 null mutant was significantly less virulent than wild-type virus in mice following intracerebral inoculation (21). In contrast, YK551 (gB-T887A) and YK553 (gB-repair) had similar LD_{50} values (Table 1). These results indicated that phosphorylation of gB Thr-887 was not required for HSV-1 virulence in mice following intracerebral inoculation.

Production and characterization of monoclonal antibodies to gB-T887^P. To directly examine the functional consequence(s) of Us3 phosphorylation of gB Thr-887 in infected cells, monoclonal antibodies were produced against a synthetic

TABLE 1. LD_{50} values of HSV-1 recombinant viruses in mice following intracerebral inoculation

Virus	LD_{50} (PFU)[a]
YK511 (Us3-K220M)	$10^{4.5}$
YK513 (Us3-repair)	$10^{1.5}$
YK551 (gB-T887A)	$10^{1.0}$
YK553 (gB-repair)	$10^{1.2}$

[a] Three-week-old female ICR mice were inoculated intracerebrally with serial 10-fold dilutions of each virus in groups of six per dilution and monitored for 14 days. LD_{50} values were determined by the Behrens-Karber method.

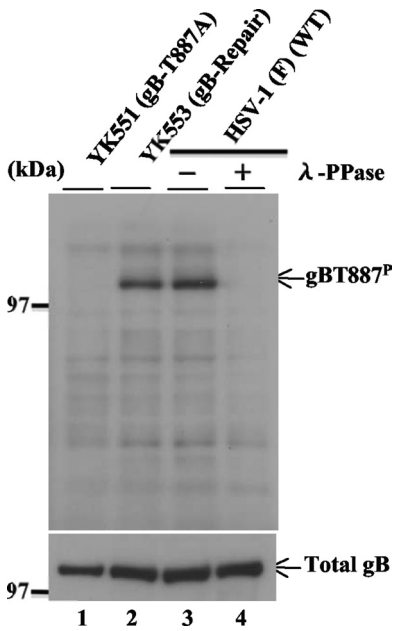

FIG. 4. Immunoblot of electrophoretically separated lysates from Vero cells infected with YK551 (gB-T887A), YK553 (gB-repair), or HSV-1 (F) at an MOI of 1. The infected Vero cells were harvested at 18 h postinfection and solubilized. The HSV-1(F)-infected Vero cell lysates were mock treated (lane 3) or treated with λ phosphatase (λ-PPase; lane 4). The infected cell lysates were then analyzed by immunoblotting with anti-gB-T887^P monoclonal antibody (upper panel) or anti-gB monoclonal antibody (lower panel).

phosphopeptide corresponding to gB residues 881 to 893 (M RKRRNTNYTQVP) in which Thr-887 was phosphorylated. Three hybridoma clones (1.46.20, 2.41.22, and 2.75.3) that secreted antibodies that reacted with the phosphopeptide but not with unphosphorylated peptide were identified by enzyme-linked immunosorbent assay and isolated. Of the three clones, clone 2.75.3 was characterized further. As shown in Fig. 4, monoclonal anti-gB-T887^P antibody reacted with wild-type HSV-1(F) gB but not with YK551 gB, which carries a T887A mutation, in immunoblots of infected Vero cell lysates. Immunoblots of lysates of Vero cells infected with YK553, in which the gB-T887A mutation in YK551 was repaired, showed restoration of the reactivity of the antibody with gB. These results indicated that the antibody recognized a gB epitope containing gB Thr-887. Furthermore, reactivity of monoclonal anti-gB-T887^P antibody with wild-type gB was dependent on phosphorylation of gB Thr-887, based on the observation that phosphatase treatment of lysates of Vero cells infected with HSV-1(F) abolished the anti-gB-T887^P antibody reactivity. Taken together, these results indicated that the anti-gB-T887^P antibody was able to specifically detect gB-T887^P in HSV-1-infected cells.

As we observed previously in Us3 immunoprecipitation assays with anti-phospho-Us3 antibody (34), the anti-gB-T887^P antibody efficiently precipitated gB from lysates of Vero cells infected with HSV-1(F) but not from lysates of Vero cells infected with HSV-1(F) treated with phosphatase or lysates of Vero cells infected with YK551 (gB-T887A) (data not shown), indicating that the anti-gB-T887^P antibody efficiently and specifically precipitated gB-T887^P from infected cell lysates. Furthermore, the efficiency of immunoprecipitation of gB from infected Vero cell lysates with anti-gB monoclonal antibody (1105) was not affected by phosphatase treatment of the lysates or by a gB-T887A mutation (data not shown), indicating that the anti-gB monoclonal antibody precipitated both phosphorylated and unphosphorylated gB proteins from infected cell lysates with similar efficiencies.

Characterization of gB-T887^P in infected cells. We previously demonstrated that phosphorylation of gB Thr-887 in infected cells was largely dependent on Us3 kinase activity, as shown by experiments using anti-phospho-PKA antibody to detect phosphorylated Thr-887 in gB purified from infected cells by immunoprecipitation (11). To confirm this result, Vero cells were mock infected or infected with wild-type HSV-1(F), YK511 (Us3-K220M), or YK513 (Us3-repair). At 18 h postinfection, infected cell lysates were analyzed by immunoblotting with anti-gB-T887^P or anti-gB antibody. In agreement with our previous study using anti-phospho-PKA substrate antibody, the amount of phosphorylated gB detected by anti-gB-T887^P antibody in the present study was dramatically reduced in YK511 (Us3-K220M)-infected cells compared to wild-type HSV-1(F)- and YK513 (Us3-repair)-infected cells (Fig. 5A). In our earlier report, we noted that phosphorylation of gB Thr-887 was slightly, but consistently, detected by the anti-phospho-PKA substrate antibody in the absence of Us3 kinase activity, suggesting that a kinase(s) other than Us3 might also phosphorylate gB Thr-887 in infected cells (11). However, in the present study, phosphorylated gB Thr-887 was not detectable by anti-gB-T887^P antibody in YK511 (Us3-K220M)-infected cells (Fig. 5A). Since anti-gB-T887^P antibody specificity for phosphorylated gB Thr-887 should be greater than that of anti-phospho-PKA substrate antibody, these results raised the possibility that phosphorylation of gB Thr-887 may be solely mediated by Us3 in infected cells.

To examine whether gB-T887^P was incorporated into virions, purified wild-type HSV-1(F) and YK551 (gB-T887A) virions were analyzed by immunoblotting with anti-gB-T887^P and anti-gB antibody. The results (Fig. 5B) showed that gB-T887^P was specifically detected in wild-type virions, indicating that gB-T887^P was incorporated into virions.

To estimate the relative amounts of total gB and gB-T887^P in infected cells, Vero cells were infected with wild-type HSV-1(F), YK551 (gB-T887A), or YK553 (gB-repair); cells were harvested at 18 h postinfection, solubilized, and immunoprecipitated with anti-gB-T887^P or anti-gB antibody. As described for the studies above, anti-gB-T887^P immunoprecipitated gB-T887^P and anti-gB immunoprecipitated phosphorylated gB, unphosphorylated gB, and gB-T887A equivalently in infected cell lysates. To obtain approximately equal amounts of immunoprecipitated gB for each of the antibodies in these experiments, fourfold dilutions of cell lysates were immunoprecipitated with anti-gB antibody and compared to the immunoprecipitates with anti-gB-T887^P antibody. The immunoprecipitates were then divided into two aliquots. Each aliquot was separated in a denaturing gel and analyzed by immunoblotting with anti-gB and anti-gB-T887^P antibody. When approximately equal amounts of total gB from HSV-1(F)- and YK553 (gB-repair)-infected cells were immunoprecipitated with anti-gB-T887^P and anti-gB antibody, the anti-gB-T887^P immunoprecipitates,

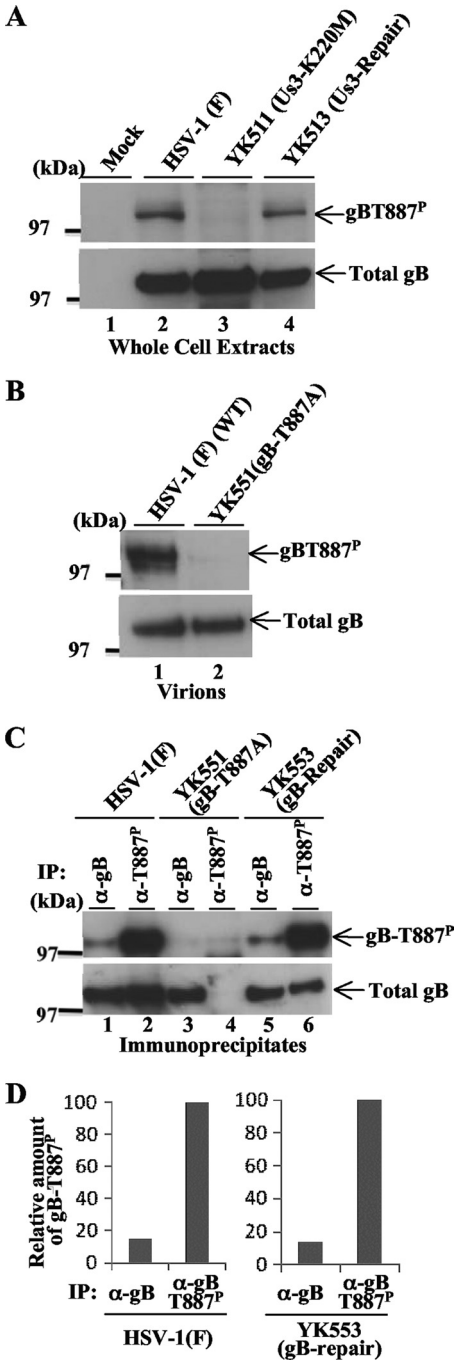

FIG. 5. (A) Immunoblots of electrophoretically separated lysates from Vero cells mock infected or infected with wild-type HSV-1(F), YK511 (Us3-K220M), or YK513 (Us3-repair) at an MOI of 1. Infected cells were harvested at 18 h postinfection and analyzed by immunoblotting with anti-gB-T887^P antibody (upper panel) or anti-gB antibody (lower panel). (B) Immunoblots of electrophoretically separated virions of wild-type HSV-1(F) (WT) or YK551 (gB-T887A) were purified by sucrose gradient centrifugation and reacted with anti-gB-T887^P antibody (upper panel) or anti-gB antibody (lower panel). (C) Immunoblots of electrophoretically separated gB immunoprecipitates from Vero cells infected with wild-type HSV-1(F) (lanes 1 and 2), YK551 (gB-T887A) (lanes 3 and 4), or YK553 (gB-repair) (lanes 5 and 6) at an MOI of 1. Infected Vero cells were harvested at 18 h postinfection, solubilized, and immunoprecipitated with anti-gB (lanes 1, 3, and 5) or anti-gB-T887^P antibody (lanes 2, 4, and 6). The immunoprecipitates (IP) were then divided into two aliquots. The aliquots of the immunoprecipitate were separated in a denaturing gel and analyzed by immunoblotting with anti-gB (upper panel) and anti-gB-T887^P antibody (lower panel). (D) Amount of gB-T887^P protein in the upper blot of panel C relative to the amount of total gB protein in the lower blot of panel C. In the left graph, the data were normalized to the relative amount for immunoprecipitates with anti-gB-T887^P antibody for cells infected with HSV-1(F) shown in lane 2 of panel C. In the right graph, the data were normalized to the relative amount for immunoprecipitates with anti-gB-T887^P antibody for cells infected with YK553 (gB-repair) shown in lane 6 of panel C. α, anti.

containing only gB-T887^P, had much more gB-T887^P than the anti-gB immunoprecipitates, which contained both phosphorylated and unphosphorylated gB Thr-887 (Fig. 5C). Quantitation of these results showed that only about 14 to 15% of total gB protein was phosphorylated at Thr-887 in cells infected with either wild-type HSV-1(F) or YK553 (gB-repair) (Fig. 5D).

The accumulation of gB-T887^P was compared to that of total gB in infected cells by infecting Vero cells with wild-type HSV-1(F) and analyzing cell lysates harvested every 3 h from 3 to 24 h postinfection by immunoblotting with anti-gB-T887^P and anti-gB antibody. There was no significant difference in the rates of accumulation of gB-T887^P and total gB in HSV-1(F)-infected cells (data not shown).

Intracellular localization of gB-T887^P in infected cells. To investigate the localization of gB-T887^P in infected cells, Vero cells were infected with HSV-1(F), YK551 (gB-T887A), or YK553 (gB-repair) and analyzed at 18 h postinfection by immunofluorescence with anti-gB-T887^P and anti-gB antibody. As shown in Fig. 6, the distribution of total gB detected by anti-gB antibody was different from that of gB-T887^P detected by anti-gB-T887^P antibody.

Cadherin, lamin B1, and PDI are markers for the plasma membrane, nuclear envelope, and endoplasmic reticulum (ER), respectively (8, 17, 37). CD71 (transferrin receptor) has been reported to be internalized in HSV-1-infected cells and to be a marker for early and recycling endosomes (2, 10). Therefore, to better resolve gB localization, wild-type HSV-1(F)-infected cells stained with anti-gB-T887^P or anti-gB antibody were also stained with anti-cadherin, anti-lamin B1, anti-PDI, or anti-CD71 antibody. In these experiments, total gB proteins colocalized with cadherin, lamin B1, and PDI while gB-T887^P colocalized with lamin B1 and PDI but not cadherin (Fig. 7). As reported previously (2), CD71 was well colocalized with total gB throughout the infected cells. In contrast, gB-T887^P was colocalized with CD71 at nuclear membrane and near perinuclear areas but not on the cell surface (Fig. 7). In addition, the frequency of CD71 colocalization with gB-T887^P in the cytoplasmic structures was lower than that with total gB. No specific staining of gB-T887^P was detected in YK551 (gB-T887A)-infected cells, and wild-type staining of gB-T887^P was restored in YK553 (gB-repair)-infected cells (Fig. 6). These results indicated that, unlike total gB, gB-T887^P was not able to be transported to and/or retained at the plasma membrane in infected cells.

Intracellular localization of total gB, gB-T887^P, and Us3 in the same infected cells. To observe the localization of total gB, gB-T887^P, and Us3 in the same cells simultaneously, Vero cells

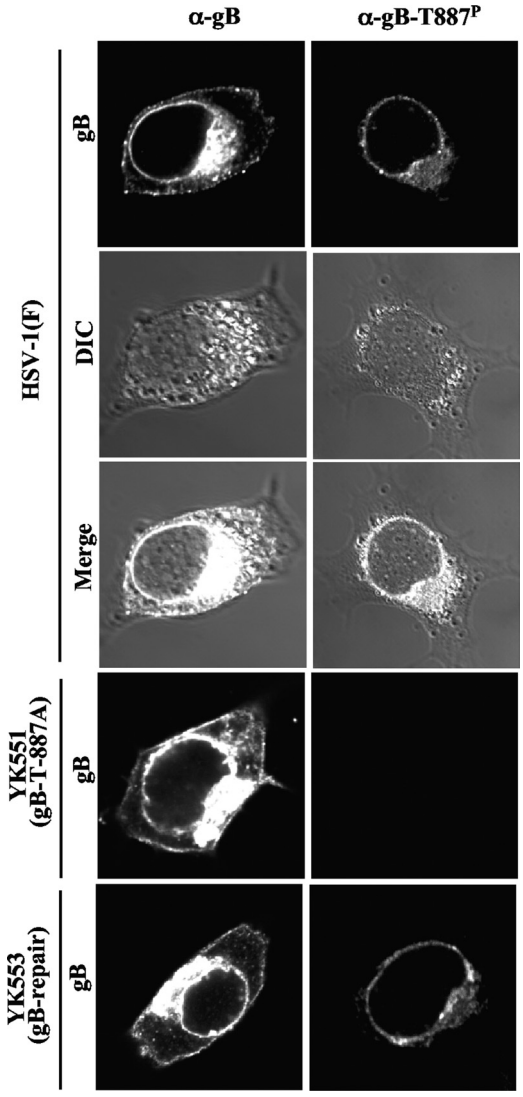

FIG. 6. Digital confocal images showing the localization of gB-T887^P. Vero cells were infected with wild-type HSV-1(F), YK551 (gB-T887A), or YK553 (gB-repair) at an MOI of 5. The infected cells were fixed at 18 h postinfection, permeabilized, stained with anti-gB-T887^P (images in right column) or anti-gB antibody (images in left column), and examined by confocal microscopy. DIC, differential interference contrast. α, anti.

were coinfected with YK501 encoding VenusA206K-Us3 and YK604 encoding ECFPA206K-gB; cells were fixed, treated with anti-gB-T887^P, and examined by confocal microscopy. YK501 (VenusA206K-Us3) grew as well as wild-type virus at MOIs of 5 and 0.01 in Vero cells (data not shown). It had been noted in similar previous studies in this and other laboratories that the anti-Us3 antibodies used in those studies had a consistent background fluorescence in the cytoplasm of cells infected with HSV-1 Us3 null mutants in immunofluorescence assays (12, 32), making it difficult to draw conclusions about the exact localization of Us3. Therefore, in this study we used YK501 (VenusA206K-Us3) to examine the localization of Us3 in infected cells. YK604 (ECFPA206K-gB) has been shown to exhibit wild-type growth properties in cell cultures and intracellular localization similar to wild-type gB in infected cells (38). As shown in Fig. 8, in Vero cells coinfected with YK501 (VenusA206K-Us3) and YK604 (ECFPA206K-gB), ECFPA 206K-gB localized at the nuclear membrane, in cytoplasmic structures, and at the plasma membrane while gB-T887^P localized at the nuclear rim and in cytoplasmic structures but not at the plasma membrane, which is in agreement with the localization of total gB and gB-T887^P in wild-type HSV-1(F)-infected cells described above (Fig. 6 and 7). VenusA206K-Us3 was detected throughout the cytoplasm, especially at the nuclear membrane, in cytoplasmic structures, and at the plasma membrane. The localization of VenusA206K-Us3 at the nuclear and plasma membranes observed in this study is consistent with the immunofluorescence studies of wild-type HSV-1-infected cells reported previously (32, 33). VenusA206K-Us3 localized with a uniform distribution at the nuclear membrane and colocalized with both ECFPA206K-gB and gB-T887^P. Similarly, VenusA206K-Us3 colocalized with both ECFPA206K-gB and gB-T887^P in some of the cytoplasmic structures. At the cell surface, VenusA206K-Us3 concentrated at several domains where ECFPA206K-gB also concentrated (Fig. 8). These results indicated that both total gB and gB-T887^P colocalized with Us3 at the nuclear membrane and in cytoplasmic structures while only unphosphorylated gB colocalized with Us3 at the cell surface in infected cells.

Phosphorylation of internalized gB from the cell surface in infected cells. To examine whether endocytosed gB was phosphorylated at Thr-887 in infected cells, the cell surface proteins of Vero cells infected with wild-type HSV-1(F) at an MOI of 1 for 18 h were biotinylated with cleavable biotin. After incubation at 37°C, the cells were treated with glutathione, harvested, and solubilized, and internalized biotinylated gB was purified by immunoprecipitation with anti-gB or anti-gB-T887^P antibody from cells and detected with streptavidin. In agreement with a previous report (2), biotinylated immunoprecipitates with anti-gB antibody from the lysate of cells incubated at 37°C for 4 h after biotinylation were detected, whereas no signal was observed with the anti-gB immunoprecipitates from cells that were treated with glutathione immediately after biotinylation (Fig. 9, lanes 1 and 2). Similar results were obtained with the anti-gB-T887^P immunoprecipitates (Fig. 9, lanes 3 and 4). These results indicated that endocytosed gB from the cell surface was phosphorylated at Thr-887 in infected cells.

DISCUSSION

We previously reported that gB Thr-887 is a physiological Us3 phosphorylation site in infected cells and that this phosphorylation appears to regulate proper expression of gB on the cell surface and may promote nuclear egress of nucleocapsids through the nuclear membrane in infected cells (11, 42). However, we have also shown that blocking gB Thr-887 phosphorylation by alanine substitution for Thr-887 had no effect on virus growth, viral cell-to-cell spread, and virus excretion to the extracellular space in cell cultures (11). Therefore, the significance of Us3 phosphorylation of gB Thr-887 and its potential effects on HSV-1 infection were uncertain. The major finding of the studies reported here is that the gB-T887A mutation significantly reduced HSV-1 replication in the mouse cornea and HSK and periocular skin disease in mice following ocular

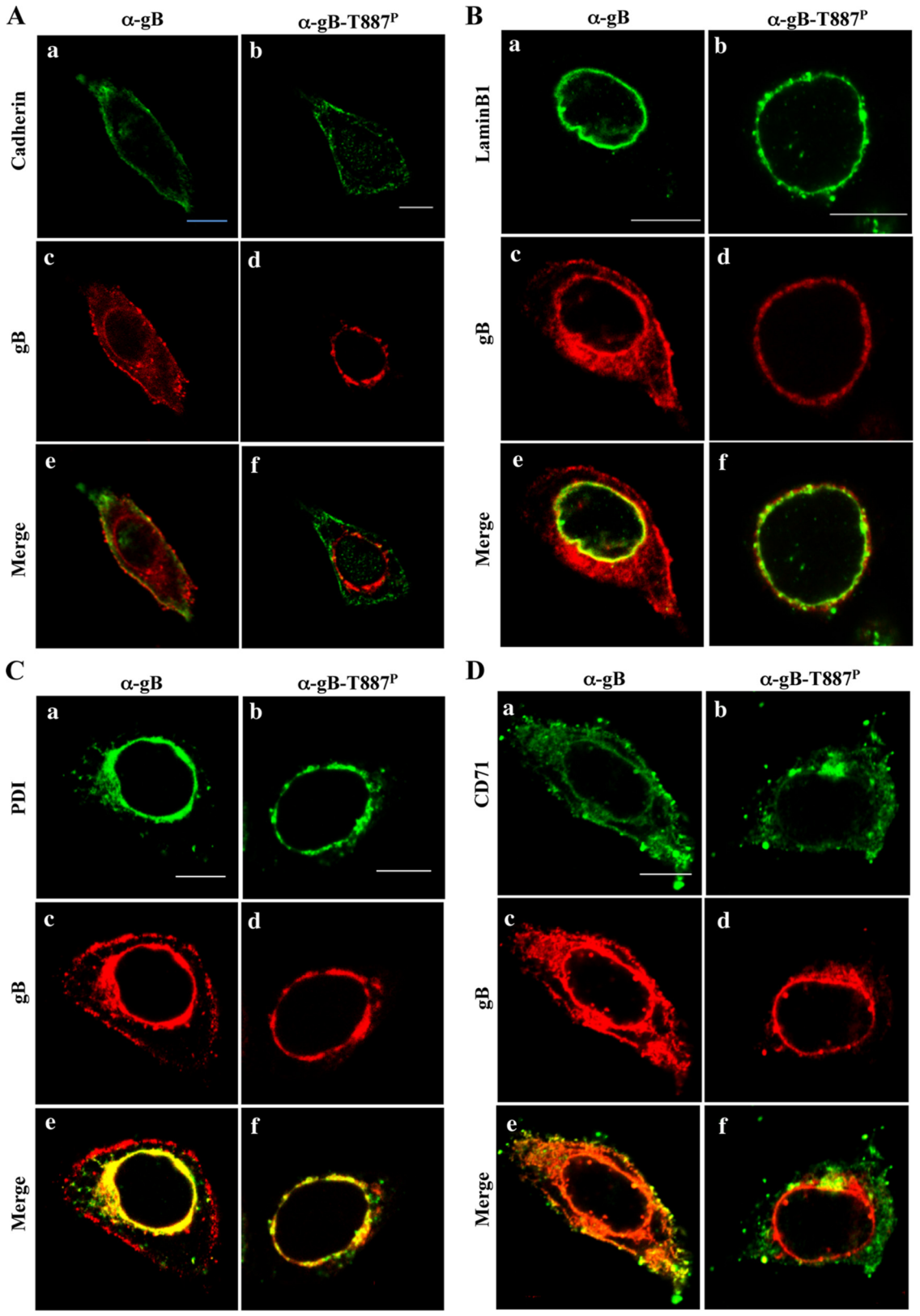

FIG. 7. Digital confocal images showing the localization of gB-T887^P. Vero cells were infected with wild-type HSV-1(F) at an MOI of 5. The infected cells were fixed at 18 h postinfection, permeabilized, stained with anti-gB-T887^P or anti-gB antibody in combination with anti-cadherin (A), lamin B1 (B), PDI (C), or CD71 (D) antibody and examined by confocal microscopy. Single-color images were captured separately and are shown in frames a to d. Frames e and f show simultaneous acquisitions of the two colors. Scale bar, 10 μm. α, anti.

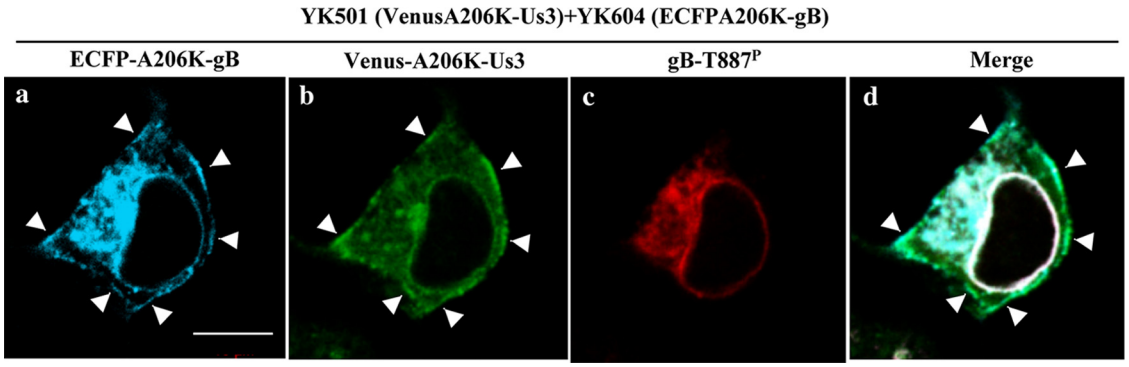

FIG. 8. Digital confocal images showing the localization of gB-T887^P. Vero cells were coinfected with YK501 (VenusA206K-Us3) and YK604 (ECFPA206K-gB) at an MOI of 5. The infected cells were fixed at 18 h postinfection, permeabilized, stained with anti-gB-T887^P, and examined by confocal microscopy. Single-color images were captured separately and are shown in frames a, b, and c. Frame d shows the simultaneous acquisition of the three colors. VenusA206K-Us3 concentrated at several domains where ECFPA206K-gB also concentrated (arrows). Scale bar, 10 μm.

infection. Similar observations were also obtained when mice were ocularly infected with YK511 encoding a Us3 kinase-inactive mutant (11). From these observations, we conclude that the effects of Us3 phosphorylation of gB Thr-887, including regulation of proper cell surface expression of gB and promotion of nuclear egress of nucleocapsids, are probably critical for HSV-1 replication and pathogenesis in vivo. However, we cannot completely eliminate the possibility that the gB-T887A mutation impairs gB function directly in vivo rather than by acting to block the Us3-mediated site of phosphorylation. For instance, it has been reported that gB is involved in the regulation of eIF-2α phosphorylation, probably by association with the eIF-2α kinase PERK (25). Although we obtained evidence that the level of phosphorylation of eIF-2α in Vero cells infected with wild-type HSV-1(F) in the absence or presence of thapsigargin, which inhibits the activity of resident $Ca2^+$-dependent chaperons in the ER and thereby induces the unfolded protein response (41), was similar to that in cells infected with YK551 (gB-T887A) (data not shown), the gB-T887A mutation might affect a reported and/or previously unreported function(s) of gB that is independent of gB phosphorylation at Thr-887.

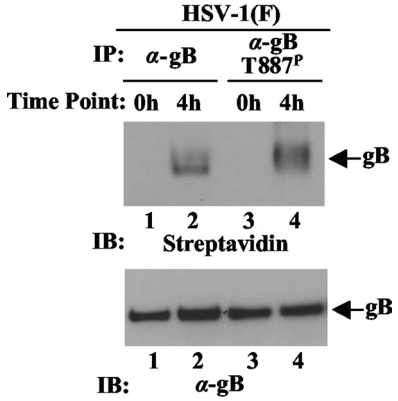

FIG. 9. Endocytosis of gB in infected cells assayed by biotinylation. Vero cells infected with wild-type HSV-1(F) at MOI of 1 for 18 h were biotinylated with sulfo-NHS-SS-cleavable biotin, incubated at 37°C for 0 or 4 h, treated with glutathione, harvested, solubilized, and immunoprecipitated with anti-gB (lanes 1 and 2) or anti-gB-T887^P antibody (lanes 3 and 4). The immunoprecipitations (IP) were subjected to immunoblotting (IB), and the biotinylated gB was detected with streptavidin. α, anti.

At present, the mechanism by which Us3 phosphorylation of gB Thr-887 contributes to viral replication and pathogenesis in vivo remains unclear. It has been reported that gB on the cell surface is a potent inducer of the immune response in vivo (4, 5, 35, 36). In fact, lysis of HSV-1-infected cells by natural killer cells has been demonstrated to correlate with cell surface expression of gB (5). However, cell surface expression of gB has been shown to be critical for viral cell-to-cell transmission (6, 15). Therefore, strict regulation of gB expression on the cell surface of infected cells may be necessary for efficient virus replication in the presence of the host immune system. Us3 phosphorylation of gB Thr-887, which can control cell surface expression of gB in infected cells, may be important for proper cell surface expression of gB, and this regulation may lead to immune evasion by infected cells in vivo. In support of this hypothesis, the studies reported here have shown differences in virus replication and pathogenesis in mice following peripheral (ocular) infections with YK551 (gB-T887A) and YK553 (gB-repair). HSV-1 virulence in mice following peripheral (ocular) infection has been considered to be significantly affected by the host immune response (7).

The molecular mechanisms by which Us3 phosphorylation of gB and UL31 affects viral infection have been investigated by mutagenesis of the Us3 substrate phosphorylation sites (11, 24). Although it is well established that mutagenesis is an effective method for investigating the functional consequences of phosphorylation of a kinase's substrates, interpretation of these results must consider the possibility that the amino acid substitution(s) might also produce a conformational change in the target protein so that the mutant's phenotype may be due to the loss of the phosphorylation site and/or to steric hindrance caused by the mutation. Therefore, a probe(s) that specifically detects the phosphorylation site(s) in the Us3 substrate in infected cells is necessary to directly determine the functional consequences of Us3 phosphorylation of its substrates in infected cells. In the present study, we developed a

monoclonal antibody (anti-gB-T887^P antibody) that specifically recognized gB-T887^P, and this antibody together with anti-gB antibody enabled us to compare localization of gB-T887^P with that of total gB in infected cells. A striking difference in localization between gB-T887^P and total gB was observed: gB-T887^P was not detectable on the cell surface of infected cells while a considerable amount of total gB was detected on the cell surface. Therefore, these studies with anti-gB-T887^P antibody presented direct evidence that Us3 phosphorylation of gB at Thr-887 regulated cell surface localization of gB in infected cells by inhibition of gB transport to and/or gB retention on the cell surface. This conclusion is in agreement with our previous observations that blocking phosphorylation of gB at Thr-887 by replacing gB Thr-887 with alanine upregulated expression of gB on the cell surface of infected cells (11). This agreement suggested that the gB-T887A mutation blocked phosphorylation of Thr-887 in gB without causing steric hindrance of the envelope protein, further supporting our conclusion, based on the studies reported here of mice infected with a recombinant virus carrying a gB-T887A mutation, that Us3 phosphorylation of gB Thr-887 played a critical role in HSV-1 replication and pathogenesis in vivo. In addition, localization of gB-T887^P at the nuclear membrane and ER and in endocytic compartments, as detected by anti-gB-T887^P antibody, suggested that gB-T887^P functions in these subcellular organelles. In particular, the localization of gB-T887^P at the nuclear membrane may support the proposal (42) that phosphorylation of gB at Thr-887 may be involved in promotion of nuclear egress of nucleocapsids through the nuclear membrane.

Immunofluorescence assays of cells coinfected with YK501 encoding VenusA206K-Us3 and YK604 encoding ECFPA206K-gB using the anti-gB-T887^P antibody showed simultaneous localization of gB-T887^P, total gB, and Us3 in the same cells. It was of particular interest that total gB colocalized with Us3 in specific domains on the cell surface at which gB-T887^P was not detectable. These observations suggested that Us3 phosphorylated gB Thr-887 at the cell surface but that this phosphorylation promoted rapid internalization of the phosphorylated protein, resulting in a barely detectable level of gB-T887^P at the cell surface. In support of this possibility, it has been reported that cell surface expression of gB in infected cells is in part regulated by endocytosis mediated by a gB tyrosine-based YTQV motif at codons 889 to 892 in its cytoplasmic tail (2). Since the Us3 phosphorylation site in gB (Thr-887) is located very close to the YTQV motif, phosphorylation of gB Thr-887 might affect the role of the YTQV motif in endocytosis. Furthermore, we presented evidence in the present study that internalized gB from the cell surface was, in fact, phosphorylated at Thr-887 in infected cells. However, we cannot eliminate the possibility that phosphorylation of gB Thr-887 inhibits transport of gB to the cell surface since Us3 colocalized with total gB and/or gB-T887^P in cytoplasmic structures in infected cells.

The anti-gB-T887^P antibody generated in these studies also enabled us to estimate the relative amounts of total gB and gB-T887^P in wild-type HSV-1(F)-infected cells. These experiments showed that only about 14 to 15% of total gB purified from wild-type HSV-1(F)-infected cells was phosphorylated at Thr-887. One hypothesis to explain this observation is that only a small fraction of gB Thr-887 is phosphorylated at any one time in infected cells; another is that there is considerable phosphorylation of gB, but this phosphorylation is transient due to rapid dephosphorylation of gB by certain phosphatase(s) and/or rapid degradation of gB with phosphorylated Thr-887 in infected cells. We prefer the latter hypothesis since loss of phosphorylation of gB Thr-887 resulted in considerable upregulation of cell surface gB expression in infected cells (11). Thus, Us3 phosphorylation of gB at Thr-887 appeared to be tightly regulated in infected cells.

ACKNOWLEDGMENTS

We thank Shihoko Koyama for excellent technical assistance.

This study was supported in part by Grants for Scientific Research and Grants for Scientific Research in Priority Areas from the Ministry of Education, Culture, Science, Sports and Technology (MEXT) of Japan and a grant from the Takeda Science Foundation.

REFERENCES

1. **Asai, R., A. Kato, K. Kato, M. Kanamori-Koyama, K. Sugimoto, T. Sairenji, Y. Nishiyama, and Y. Kawaguchi.** 2006. Epstein-Barr virus protein kinase BGLF4 is a virion tegument protein that dissociates from virions in a phosphorylation-dependent process and phosphorylates the viral immediate-early protein BZLF1. J. Virol. **80:**5125–5134.
2. **Beitia Ortiz de Zarate, I., L. Cantero-Aguilar, M. Longo, C. Berlioz-Torrent, and F. Rozenberg.** 2007. Contribution of endocytic motifs in the cytoplasmic tail of herpes simplex virus type 1 glycoprotein B to virus replication and cell-cell fusion. J. Virol. **81:**13889–13903.
3. **Benetti, L., and B. Roizman.** 2004. Herpes simplex virus protein kinase US3 activates and functionally overlaps protein kinase A to block apoptosis. Proc. Natl. Acad. Sci. U. S. A. **101:**9411–9416.
4. **Bishop, G. A., J. C. Glorioso, and S. A. Schwartz.** 1983. Relationship between expression of herpes simplex virus glycoproteins and susceptibility of target cells to human natural killer activity. J. Exp. Med. **157:**1544–1561.
5. **Bishop, G. A., S. D. Marlin, S. A. Schwartz, and J. C. Glorioso.** 1984. Human natural killer cell recognition of herpes simplex virus type 1 glycoproteins: specificity analysis with the use of monoclonal antibodies and antigenic variants. J. Immunol. **133:**2206–2214.
6. **Cai, W. H., B. Gu, and S. Person.** 1988. Role of glycoprotein B of herpes simplex virus type 1 in viral entry and cell fusion. J. Virol. **62:**2596–2604.
7. **Carr, D. J., P. Harle, and B. M. Gebhardt.** 2001. The immune response to ocular herpes simplex virus type 1 infection. Exp. Biol. Med. (Maywood) **226:**353–366.
8. **Ellgaard, L., and L. W. Ruddock.** 2005. The human protein disulphide isomerase family: substrate interactions and functional properties. EMBO Rep. **6:**28–32.
9. **Frame, M. C., F. C. Purves, D. J. McGeoch, H. S. Marsden, and D. P. Leader.** 1987. Identification of the herpes simplex virus protein kinase as the product of viral gene US3. J. Gen. Virol. **68:**2699–2704.
10. **Grant, B. D., and J. G. Donaldson.** 2009. Pathways and mechanisms of endocytic recycling. Nat. Rev. Mol. Cell Biol. **10:**597–608.
11. **Kato, A., J. Arii, I. Shiratori, H. Akashi, H. Arase, and Y. Kawaguchi.** 2009. Herpes simplex virus 1 protein kinase Us3 phosphorylates viral envelope glycoprotein B and regulates its expression on the cell surface. J. Virol. **83:**250–261.
12. **Kato, A., M. Tanaka, M. Yamamoto, R. Asai, T. Sata, Y. Nishiyama, and Y. Kawaguchi.** 2008. Identification of a physiological phosphorylation site of the herpes simplex virus 1-encoded protein kinase Us3 which regulates its optimal catalytic activity in vitro and influences its function in infected cells. J. Virol. **82:**6172–6189.
13. **Kato, A., M. Yamamoto, T. Ohno, H. Kodaira, Y. Nishiyama, and Y. Kawaguchi.** 2005. Identification of proteins phosphorylated directly by the Us3 protein kinase encoded by herpes simplex virus 1. J. Virol. **79:**9325–9331.
14. **Kawaguchi, Y., C. Van Sant, and B. Roizman.** 1997. Herpes simplex virus 1 alpha regulatory protein ICP0 interacts with and stabilizes the cell cycle regulator cyclin D3. J. Virol. **71:**7328–7336.
15. **Laquerre, S., R. Argnani, D. B. Anderson, S. Zucchini, R. Manservigi, and J. C. Glorioso.** 1998. Heparan sulfate proteoglycan binding by herpes simplex virus type 1 glycoproteins B and C, which differ in their contributions to virus attachment, penetration, and cell-to-cell spread. J. Virol. **72:**6119–6130.
16. **Leach, N., S. L. Bjerke, D. K. Christensen, J. M. Bouchard, F. Mou, R. Park, J. Baines, T. Haraguchi, and R. J. Roller.** 2007. Emerin is hyperphosphorylated and redistributed in herpes simplex virus type 1-infected cells in a manner dependent on both UL34 and US3. J. Virol. **81:**10792–10803.
17. **Leckband, D., and A. Prakasam.** 2006. Mechanism and dynamics of cadherin adhesion. Annu. Rev. Biomed. Eng. **8:**259–287.

18. **Leopardi, R., C. Van Sant, and B. Roizman.** 1997. The herpes simplex virus 1 protein kinase US3 is required for protection from apoptosis induced by the virus. Proc. Natl. Acad. Sci. U. S. A. **94:**7891–7896.
19. **Maresova, L., T. J. Pasieka, E. Homan, E. Gerday, and C. Grose.** 2005. Incorporation of three endocytosed varicella-zoster virus glycoproteins, gE, gH, and gB, into the virion envelope. J. Virol. **79:**997–1007.
20. **McGeoch, D. J., and A. J. Davison.** 1986. Alphaherpesviruses possess a gene homologous to the protein kinase gene family of eukaryotes and retroviruses. Nucleic Acids Res. **14:**1765–1777.
21. **Meignier, B., R. Longnecker, P. Mavromara-Nazos, A. E. Sears, and B. Roizman.** 1988. Virulence of and establishment of latency by genetically engineered deletion mutants of herpes simplex virus 1. Virology **162:**251–254.
22. **Morris, J. B., H. Hofemeister, and P. O'Hare.** 2007. Herpes simplex virus infection induces phosphorylation and delocalization of emerin, a key inner nuclear membrane protein. J. Virol. **81:**4429–4437.
23. **Mou, F., T. Forest, and J. D. Baines.** 2007. US3 of herpes simplex virus type 1 encodes a promiscuous protein kinase that phosphorylates and alters localization of lamin A/C in infected cells. J. Virol. **81:**6459–6470.
24. **Mou, F., E. Wills, and J. D. Baines.** 2009. Phosphorylation of the U_L31 protein of herpes simplex virus 1 by the U_S3-encoded kinase regulates localization of the nuclear envelopment complex and egress of nucleocapsids. J. Virol. **83:**5181–5191.
25. **Mulvey, M., C. Arias, and I. Mohr.** 2007. Maintenance of endoplasmic reticulum (ER) homeostasis in herpes simplex virus type 1-infected cells through the association of a viral glycoprotein with PERK, a cellular ER stress sensor. J. Virol. **81:**3377–3390.
26. **Munger, J., A. V. Chee, and B. Roizman.** 2001. The U_S3 protein kinase blocks apoptosis induced by the *d*120 mutant of herpes simplex virus 1 at a premitochondrial stage. J. Virol. **75:**5491–5497.
27. **Munger, J., and B. Roizman.** 2001. The US3 protein kinase of herpes simplex virus 1 mediates the posttranslational modification of BAD and prevents BAD-induced programmed cell death in the absence of other viral proteins. Proc. Natl. Acad. Sci. U. S. A. **98:**10410–10415.
28. **Ogg, P. D., P. J. McDonell, B. J. Ryckman, C. M. Knudson, and R. J. Roller.** 2004. The HSV-1 Us3 protein kinase is sufficient to block apoptosis induced by overexpression of a variety of Bcl-2 family members. Virology **319:**212–224.
29. **Purves, F. C., R. M. Longnecker, D. P. Leader, and B. Roizman.** 1987. Herpes simplex virus 1 protein kinase is encoded by open reading frame US3 which is not essential for virus growth in cell culture. J. Virol. **61:**2896–2901.
30. **Purves, F. C., D. Spector, and B. Roizman.** 1991. The herpes simplex virus 1 protein kinase encoded by the US3 gene mediates posttranslational modification of the phosphoprotein encoded by the UL34 gene. J. Virol. **65:**5757–5764.
31. **Reynolds, A. E., B. J. Ryckman, J. D. Baines, Y. Zhou, L. Liang, and R. J. Roller.** 2001. U_L31 and U_L34 proteins of herpes simplex virus type 1 form a complex that accumulates at the nuclear rim and is required for envelopment of nucleocapsids. J. Virol. **75:**8803–8817.
32. **Reynolds, A. E., E. G. Wills, R. J. Roller, B. J. Ryckman, and J. D. Baines.** 2002. Ultrastructural localization of the herpes simplex virus type 1 UL31, UL34, and US3 proteins suggests specific roles in primary envelopment and egress of nucleocapsids. J. Virol. **76:**8939–8952.
33. **Ryckman, B. J., and R. J. Roller.** 2004. Herpes simplex virus type 1 primary envelopment: UL34 protein modification and the US3-UL34 catalytic relationship. J. Virol. **78:**399–412.
34. **Sagou, K., T. Imai, H. Sagara, M. Uema, and Y. Kawaguchi.** 2009. Regulation of the catalytic activity of herpes simplex virus 1 protein kinase Us3 by autophosphorylation and its role in pathogenesis. J. Virol. **83:**5773–5783.
35. **Sanchez-Pescador, L., P. Paz, D. Navarro, L. Pereira, and S. Kohl.** 1992. Epitopes of herpes simplex virus type 1 glycoprotein B that bind type-common neutralizing antibodies elicit type-specific antibody-dependent cellular cytotoxicity. J. Infect. Dis. **166:**623–627.
36. **Sanchez-Pescador, L., L. Pereira, E. D. Charlebois, and S. Kohl.** 1993. Antibodies to epitopes of herpes simplex virus type 1 glycoprotein B (gB) in human sera: analysis of functional gB epitopes defined by inhibition of murine monoclonal antibodies. J. Infect. Dis. **168:**844–853.
37. **Stuurman, N., S. Heins, and U. Aebi.** 1998. Nuclear lamins: their structure, assembly, and interactions. J. Struct. Biol. **122:**42–66.
38. **Sugimoto, K., M. Uema, H. Sagara, M. Tanaka, T. Sata, Y. Hashimoto, and Y. Kawaguchi.** 2008. Simultaneous tracking of capsid, tegument, and envelope protein localization in living cells infected with triply fluorescent herpes simplex virus 1. J. Virol. **82:**5198–5211.
39. **Tanaka, M., H. Kagawa, Y. Yamanashi, T. Sata, and Y. Kawaguchi.** 2003. Construction of an excisable bacterial artificial chromosome containing a full-length infectious clone of herpes simplex virus type 1: viruses reconstituted from the clone exhibit wild-type properties in vitro and in vivo. J. Virol. **77:**1382–1391.
40. **Tanaka, M., Y. Nishiyama, T. Sata, and Y. Kawaguchi.** 2005. The role of protein kinase activity expressed by the UL13 gene of herpes simplex virus 1: the activity is not essential for optimal expression of UL41 and ICP0. Virology **341:**301–312.
41. **Treiman, M., C. Caspersen, and S. B. Christensen.** 1998. A tool coming of age: thapsigargin as an inhibitor of sarco-endoplasmic reticulum Ca(2+)-ATPases. Trends Pharmacol. Sci. **19:**131–135.
42. **Wisner, T. W., C. C. Wright, A. Kato, Y. Kawaguchi, F. Mou, J. D. Baines, R. J. Roller, and D. C. Johnson.** 2009. Herpesvirus gB-induced fusion between the virion envelope and outer nuclear membrane during virus egress is regulated by the viral US3 kinase. J. Virol. **83:**3115–3126.